Mat. Res. Soc. Symp. Proc. Vol. 740 © 2003 Materials Research Society

Tensile Deformation and Fatigue Crack Growth in Bulk Nanocrystalline Al-7.5Mg

P.S. Pao, H.N. Jones, S.J. Gill, and C. R. Feng
Materials Science and Technology Division, Naval Research Laboratory
Washington, DC 20375, U.S.A.

ABSTRACT

The fatigue crack growth kinetics and tensile deformation of bulk nanocrystalline Al-7.5Mg were investigated. Nanocrystalline particulates were first prepared by mechanically ball milling spray atomized Al-7.5Mg powders in liquid nitrogen. These particulates were then degassed, consolidated by hot isostatic pressing, and extruded into rods. Bulk nanocrystalline Al-7.5Mg has significantly higher fatigue crack growth rates and lower fatigue crack growth thresholds than those of ingot-processed 7050-T7451. The fatigue crack growth thresholds exhibit only a weak stress ratio dependency and can be identified as having a Class I behavior when using the fatigue classification proposed by Vasudevan and Sadananda. In 3.5% NaCl solution, fatigue crack growth rates of bulk nanocrystalline Al-7.5Mg are as much as three times higher than those obtained in air. Tensile fracture of bulk nanocrystalline Al-7.5Mg is preceded by the formation of a localized shear band. In contrast to the low dislocation density in the as-extruded material, the gage section and the shear band region both exhibited a high dislocation density and dislocation cell structure.

INTRODUCTION

Nanocrystalline materials have received considerable attention recently due to the possibility of improved surface, electronic, optical, magnetic, and/or mechanical properties. Because of the difficulties in producing nanocrystalline materials in sufficiently large quantity and quality, however, many studies on nanocrystalline materials have been limited to thin films or very small samples. Mechanical properties of nanocrystalline materials have thus often been deduced indirectly from indentation tests due to the limited amount available. With recent advances in nanocrystalline materials production techniques, such as ball milling at cryogenic temperatures (cryomilling), large quantities of Al-Mg particulates with grain sizes of several nanometers can be successfully produced [1-5]. Good tensile strength and creep properties have been demonstrated for bulk nanocrystalline Al-Mg alloys [1,2]. However, the fatigue crack growth behavior and the effect of very small grain size on the fatigue crack growth kinetics of bulk nanocrystalline aluminum alloys have not been established.

In the present study, the fatigue crack growth kinetics and tensile deformation behavior of a bulk nanocrystalline Al-Mg alloy were determined. The fatigue crack growth rates and fatigue crack growth threshold stress intensity factor ranges (ΔK_{th}) of a bulk nanocrystalline Al-Mg alloy in both air and 3.5% NaCl solution were evaluated and were compared to those of ingot-metallurgy large grained alloy.

EXPERIMENTAL PROCEDURES

The bulk nanocrystalline material used in this study was 101.6-mm-diameter Al-7.5Mg extruded rod. Spray atomized Al-7.5Mg powders with a particle size less than 100 μm were mechanically ball milled in liquid nitrogen for eight hours. Details of the cryomilling processes can be found in [6]. The cryomilled powders were degassed at 317 °C in a 1.33×10^{-4} Pa vacuum, consolidated by hot isostatic pressing (HIP) at 317 °C and 200 MPa, and then extruded at 202 °C into an 101.6-mm-diameter rod with an extrusion ratio of 6.5:1.

For fatigue crack growth studies, 5.08-mm-thick compact-tension (CT) specimens with a width of 38.1 mm and oriented in the C-R direction were machined from as-extruded Al-7.5Mg rod. Fatigue crack growth tests were performed in ambient air (20 °C and 42% relative humidity) and in a flowing 3.5% NaCl solution (exposed to air under an open-circuit condition) at a cyclic load frequency of 5 Hz using a sine waveform and load ratios from 0.1 to 0.8. Details of the fatigue crack growth test procedures can be found in [7]. After fatigue tests, the fatigue-fractured surfaces were studied by scanning electron microscopy (SEM). A profilometer was used to measure the fracture surface roughness of the post-fatigue specimens. Transmission electron microscopy (TEM) was performed to examine dislocation structures.

RESULTS

Microstructures and tensile deformation

The grain size of the as-cryomilled Al-7.5Mg powders was not determined in this study. However, based on the work done at UC-Irvine on a similar alloy under identical cryomilling conditions, the average grain size of the as-cryomilled Al-7.5Mg powders was estimated to be about 25 nm. Following elevated temperature degassing, HIP, and extrusion, the grains coarsened considerably to an average size of about 250 nm. Even though the grains grew during powder processing and extrusion, the average grain size of the bulk nanocrystalline Al-7.5Mg was still more than two orders-of-magnitude smaller than that of typical ingot-metallurgy aluminum alloys. The Al-7.5Mg extrusion also contained sharp fiber texture with {111} planes parallel to the extrusion direction.

Table 1: Tensile Properties of Aluminum Alloys

Material	Yield Strength (MPa)	Tensile Strength (MPa)	% elongation
Al-7.5Mg	553	665	4.2
Al 5083-H321	228	317	16.0
Al 7050-T74	455	510	11.0

Tensile properties in the longitudinal direction (parallel to the extrusion direction) of bulk nanocrystalline Al-7.5Mg are tabulated in Table 1, together with those of ingot-metallurgy Al 5083-H321 (Al-4.4Mg-0.7Mn-0.15Cr) and Al 7050-T74 (Al-6.2Zn-2.25Mg-2.3Cu-0.12Zr). As shown in Table 1, the yield strength of bulk nanocrystalline Al-7.5Mg is more than twice that of Al 5083-H321, and is about 100 MPa more than that of high-strength Al-7050-T74. The tensile

elongation of the bulk nanocrystalline Al-7.5Mg, however, is significantly lower than those of both Al 5083-H321 and Al 7050-T74.

The onset of tensile instability occurred at plastic strains on the order of 0.7% and consisted of the sudden formation of a macroscopic shear band, usually near one of the shoulders of the test specimen. Any further straining beyond this point would induce a flat transverse fracture at the shear band location surrounded by 0.76 mm thick shear lips with a local reduction in area of about 6%. Due to the limited tensile deformation ductility of this material compression tests were conducted to further investigate its deformation behavior. Samples were cut from the undamaged portions of grip section of the tension test specimens. These were then tested in compression at strain rates of 10^{-4} s^{-1} and 10^{-3} s^{-1} between hardened platens in a servohydraulic load frame using a molydisulfide lubricant to reduce barreling of the sample.

The flow behavior of this material in compression exhibited two unusual effects. At plastic strains between 0.8% and 3% the work hardening rate was slightly negative. In addition the flow stress at 10^{-4} s^{-1} was greater by 7 MPa on average than that at 10^{-3} s^{-1} indicating a small negative strain rate sensitivity. These two aspects of the deformation behavior of the material cause it to exhibit a low tensile ductility. While there is evidence of a higher dislocation density in the gage section and the shear band region, the dislocation storage efficiency at plastic strains above 0.8% must be low to account for the low work hardening rate.

Fatigue crack growth kinetics

Fatigue crack growth rates as a function of stress-intensity-factor-range (ΔK) in an ambient air for bulk nanocrystalline Al-7.5Mg are shown in Fig. 1a. Fatigue crack growth rates of ingot-metallurgy Al 7050-T74 under similar test conditions are also included in Fig. 1a for comparison. The fatigue crack growth rate data of Al-7.5Mg exhibits the typical sigmoidal shape in the log-log plot, and can be separated into a near-threshold Stage I and an intermediate Stage II.

As shown in Fig. 1a, in ambient air and at intermediate and high ΔK, the fatigue crack growth rates of Al-7.5Mg are three to five times higher than those of Al 7050-T74 at comparable ΔK. Furthermore, the apparent ΔK_{th} of Al-7.5Mg is only about 1 MPa $\sqrt{m}$, which is significantly lower than the 2.2 MPa $\sqrt{m}$ exhibited by Al 7050-T74. As will be discussed later, the higher fatigue crack growth rates and lower ΔK_{th} of Al-7.5Mg can be attributed to the much smoother fracture surfaces which led to much lower fracture surface roughness induced crack closure levels when compared to Al 7050-T74.

Figure 1b compares the fatigue crack growth rates of Al-7.5Mg in a 3.5% NaCl solution to those obtained in ambient air. As shown in Fig. 1b, at high ΔK, the fatigue crack growth rates in a 3.5% NaCl solution are up to three times faster than those in air. As ΔK decreases, however, the difference between fatigue crack growth rates obtained in a 3.5% NaCl solution and in air progressively diminishes. At ΔK slightly above 2 MPa $\sqrt{m}$, the fatigue crack growth rates are essentially the same in these two environments and the apparent ΔK_{th} in a 3.5% NaCl solution is slightly less than 2 MPa $\sqrt{m}$. That is, the apparent ΔK_{th} observed in a more aggressive 3.5% NaCl solution is actually significantly higher than that obtained in ambient air. This seemingly contradictory behavior is also observed in ingot-metallurgy 2000- and 7000-series alloys and can be attributed to the corrosion product induced crack closure phenomenon which can effectively reduce the crack tip opening driving force and cause apparently higher ΔK_{th} [7,8].

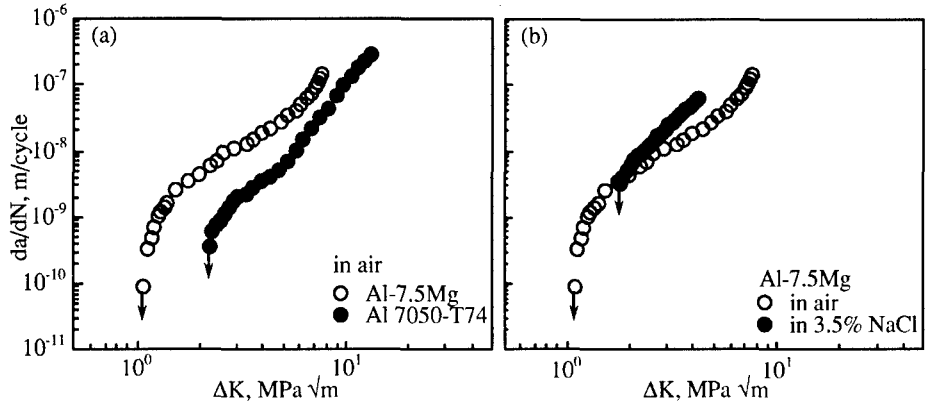

Figure 1. (a) Comparison of fatigue crack growth in air of Al-7.5Mg and Al 7050-T74 and (b) Effect of environment on fatigue crack growth of Al-7.5Mg.

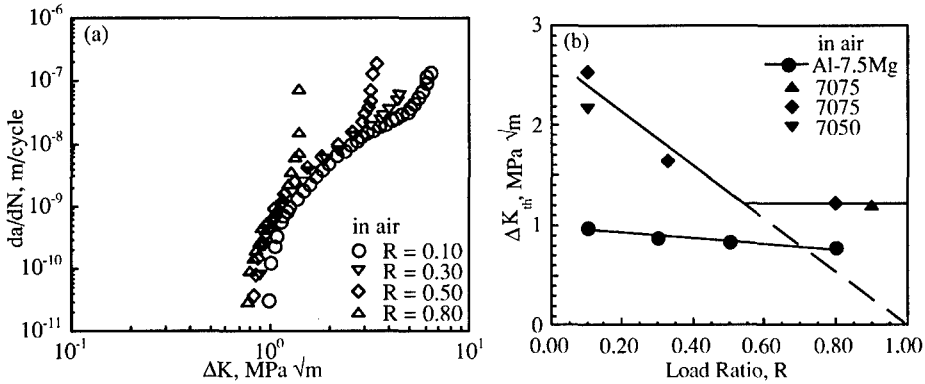

Figure 2. (a) Fatigue crack growth in air of Al-7.5Mg and (b) Effect of load ratio on fatigue crack growth thresholds of Al-7.5Mg, Al 7075, and Al 7050.

To take advantage of the recently developed classification of fatigue crack growth behavior and to elucidate the effect of load ratio on fatigue crack growth, fatigue crack growth kinetics of nanocrystalline Al-7.5Mg in air at load ratios from 0.1 to 0.8 are determined and are shown in Fig. 2a. As shown in Fig. 2a, fatigue crack growth rate curve at each load ratio follows a sigmoidal shape. While there are large divergences at high ΔK, where crack growth approaches instability, the differences in ΔK_{th} are actually small. The effect of load ratio on ΔK_{th} is shown in Fig. 2b together with the data from 7000-series ingot alloys. As shown in Fig. 2b, the fatigue crack growth thresholds of Al-7.5Mg exhibit only weak load ratio dependency and can be

identified as having a Class I behavior when using the fatigue classification proposed by Vasudevan and Sadananda [9]. In contrast, ingot 7000-series alloys exhibit a Class III behavior as their fatigue crack growth thresholds demonstrate strong load ratio dependence from R = 0.1 to 0.5, but remain independent of load ratio at R > 0.5.

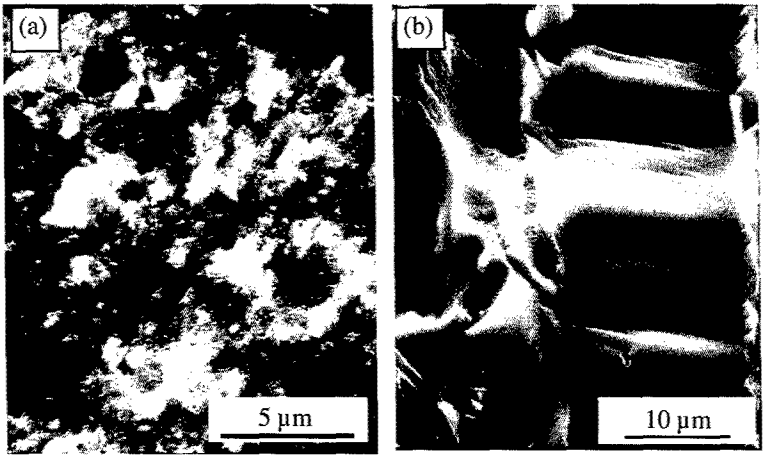

Figure 3. Fatigue fracture surface morphology in air of (a) Al-7.5Mg (at $\Delta K = 1.1$ MPa $\sqrt{m}$) and (b) Al 7050-T74 (at $\Delta K = 2.2$ MPa $\sqrt{m}$).

Figures 3a and 3b compare, respectively, the fatigue fracture surface morphologies of bulk nanocrystalline Al-7.5Mg and Al 7050-T74, both taken in the near-threshold region in an ambient air environment. As shown in Fig. 3b, the fracture surface morphology of Al 7050-T74 is very rough and fracture paths are transgranular and highly tortuous. Many crystallographic steps can be seen across the large elongated pancake grains and some slip traces are also present on these steps. The average surface roughness as measured by profilometer is 24 μm. In contrast, as shown in Fig. 3a, the fatigue fracture surface morphology produced in ambient air of bulk nanocrystalline Al-7.5Mg is largely uncharacteristic with no apparent crystallographic features. The fracture surfaces, even in the near-threshold region of the bulk nanocrystalline Al-7.5Mg, are much smoother than those of Al 7050-T74. The average surface roughness of the bulk nanocrystalline Al-7.5Mg as measured by profilometer is about 0.8 μm, which is thirty times smaller than the 24 μm observed in Al 7050-T74.

The observed difference in fatigue crack growth kinetics in air between the bulk nanocrystalline Al-7.5Mg and Al 7050-T74, as shown in Fig. 1a, therefore, can be attributed largely to the difference in fracture surface roughness induced crack closure levels in these two alloys. The crack closure levels in Al 7050-T74 are significantly higher than those exhibited by Al-7.5Mg. For instance, the crack closure level in the near-threshold region of Al 7050-T74 is about 43% of the maximum applied load whereas it is almost zero for the Al-7.5Mg. If the stress-intensity factor is truncated to account for roughness-induced crack closure and the

effective stress-intensity-factor-range ΔK_{eff} is used as a measure of the fatigue crack driving force, then the difference between the fatigue crack growth rates and the ΔK_{th} is significantly reduced.

SUMMARY

Fatigue crack growth rates through bulk nanocrystalline Al-7.5Mg are significantly higher and the fatigue crack growth thresholds are significantly lower than those of ingot-metallurgy Al 7050-T74. The higher fatigue crack growth rates and lower thresholds can be attributed to the much smoother fracture surface morphology and lower roughness induced crack closure in bulk nanocrystalline Al-7.5Mg. The fatigue crack growth thresholds in air exhibit only a weak stress ratio dependency and can be identified as having a Class I behavior when using the fatigue classification proposed by Vasudevan and Sadananda. At intermediate and high stress intensities, fatigue crack growth rates of bulk nanocrystalline Al-7.5Mg in 3.5% NaCl solution are higher than those obtained in air.

ACKNOWLEDGEMENTS

This work was supported by the Office of Naval Research, and monitored by Dr. A.J. Sedriks. Special thanks are extended to Dr. K. Sadananda of NRL for many helpful discussions, and to Dr. Dan Matejczyk of Boeing and Professor Enrique Lavernia of UC-Irvine for providing bulk nanocrystalline Al-7.5Mg extruded rod.

REFERENCES

1. R. Hayes, V. Tellkamp, and E. Lavernia, Scripta Materialia 41, 743 (1999).
2. V.L. Tellkamp and E.J. Lavernia, Nanostruct. Mater. 12, 249 (1999).
3. J. Rawers, G. Slavens, and R. Krabbe, Nanostruct. Mater. 9, 197 (1997).
4. R.J. Perez, H.G. Jiang, and E.J. Lavernia, Nanostruct. Mater. 9, 71 (1997).
5. M.J. Lau, H.G. Jiang, R.J. Perez, J. Juarez-Islas, and E.J. Lavernia, Nanostruct. Mater. 9, 157 (1997).
6. R.J. Perez, B. Huang, and E.J. Lavernia, Nanostruct. Mater. 7, 565 (1996).
7. P.S. Pao, S.J. Gill, C.R. Feng, and K.K. Sankaran, Scripta Materialia 45, 605 (2001).
8. P.S. Pao, M.A. Imam, L.A. Cooley, and G.R. Yoder, Corrosion 45, 530 (1989).
9. A.K. Vasudevan and K. Sadananda, Metall. Trans. 26A, 1221 (1995).